

Effect of style of faulting on the orientation of maximum horizontal earthquake response spectra

Alan Poulos^{*1} and Eduardo Miranda¹

¹Department of Civil and Environmental Engineering, Stanford University,
Stanford, California, U.S.A.

Abstract

Horizontal earthquake ground motions have intensities that vary with changes in orientation, that is, they depend on the azimuth. Previous studies have found that the maximum horizontal spectral acceleration at mid-to-long periods is more likely to be closer to the strike-normal orientation than to the strike parallel orientation for ground motions recorded very close to earthquake ruptures. However, this trend disappears relatively quickly as the distance to the rupture increases and becomes almost nonexistent for rupture distances longer than 5 km. Using a database of ground motions from shallow crustal earthquakes in active tectonic regimes, this work studies the orientation of maximum horizontal spectral acceleration of ground motions from earthquakes with strike-slip and reverse faulting. For strike-slip earthquakes, these orientations of maximum intensity are found to be close to the transverse orientation, i.e., an orientation that is perpendicular to the line segment between the recording station and the earthquake epicenter. Contrary to what occurs with respect to the previously studied strike-normal orientation, the orientation of maximum spectral response remains close to the transverse orientation regardless of source-to-site distance. Moreover, on average, the orientations of maximum spectral response tend to become closer to the transverse orientation as the period increases. On the other hand, ground motions from reverse earthquakes do not show any trend in the orientation of maximum spectral response relative to the transverse orientation. Probability distributions of the angular difference between the orientation of maximum spectral response and the transverse orientation for strike-slip earthquakes were fitted at several periods between 0.01 and 10 s. These directionality effects from strike-slip earthquakes could be considered in future seismic hazard analyses.

*Corresponding author: apoulos@stanford.edu

Introduction

Traditionally, Ground Motion Models (GMM) have provided an estimate of a scalar measure of horizontal earthquake response spectra at a site, whose ordinates at a given period usually correspond to a measure of central tendency such as the median intensity from all horizontal orientations (usually referred to as RotD50, Boore, 2010). However, ground motion intensities, such as response spectral ordinates, can vary significantly with changes in orientation within the horizontal plane (i.e., with changes in azimuth), a phenomenon known as directionality. For example, 5% damped spectral ordinates at 1 s are, on average, 55% higher in the orientation of maximum intensity within the horizontal plane than in the perpendicular orientation, and longer periods of vibration have even larger differences in intensity (Poulos and Miranda, 2022). Most studies have concentrated on quantifying directionality by computing ratios between different definitions of horizontal spectral acceleration (e.g., Beyer and Bommer, 2006; Campbell and Bozorgnia, 2008; Huang et al., 2008; Boore and Kishida, 2017), such as the ratio between the maximum spectral acceleration within the horizontal plane (usually referred to as RotD100, Boore, 2010) and RotD50. However, much less attention has been devoted to studying the orientations at which the maximum intensities occur.

Ground motion directionality has received significant attention in the engineering community particularly after the 1994 M_w 6.7 Northridge earthquake due to concerns regarding strong polarization caused by forward directivity in the near-source region. Somerville et al. (1997) found that spectral accelerations at periods longer than 0.6 s were systematically larger in the strike-normal orientation than in the strike-parallel orientation for sites that are close to the source. Somerville (2003) later modeled forward directivity in the strike-normal orientation as a narrow band velocity pulse with a period that increases with earthquake magnitude. However, using the NGA ground motion database, Watson-Lamprey and Boore (2007) found that the orientation of maximum spectral acceleration rarely coincides with the strike-normal orientation, especially for source-to-site distances greater than 3 km. Even for ground motions very near to the source, Howard et al. (2005) found that the orientation that maximizes the mean response spectrum for periods between 0.5 and 3 s, and hence also maximizes the Housner spectral intensity (Housner, 1952), differs from the strike-normal orientation. Using a relatively small sample of 15 ground motions with strike-slip faulting and 14 ground motions with reverse faulting they found mean differences between the orientation of largest spectral intensity and the strike-normal orientation of 21° and 29°, respectively.

More recently, Shahi and Baker (2014) used the NGA-West2 ground motion database to show that the angle between the orientation of maximum intensity and the fault strike was essentially random, having a practically uniform probability distribution except for oscillators with periods of vibration longer than 1 s and source-to-site distances less than 5 km, where they observed a greater likelihood of the orientation of maximum intensity to be closer to the strike-normal orientation than to the fault-parallel orientation. Bradley and Baker (2015) conducted a similar analysis of the directionality of ground motions recorded in 20 recording stations within the Christchurch urban area during 10 events of the 2010–2011 Canterbury, New Zealand earthquakes. Consistent with findings by Shahi and Baker (2014), they found that when averaging the results from all stations during all events and for 20 vibration periods between 0.01 and 10 s, the angle between the orientation of maximum intensity and the fault strike was uniformly distributed, that is, lacking a predominant orientation in which the maximum intensity occurs relative to the fault strike. However, they also found that for oscillators with periods longer than 1 s subjected the 2010 M_w

7.1 Darfield earthquake records, the orientations of maximum intensity were much closer to the strike-normal than to the strike-parallel orientation, with all studied station having an average angle between the orientation of maximum intensity and the fault strike higher than 45° . The recording stations that they considered were located at rupture distances up to approximately 30 km, notably higher than the 5 km from [Shahi and Baker \(2014\)](#), suggesting that directionality effects can also occur at longer distances.

Orientations of maximum ground motion intensity have also been studied for other types of intensities (i.e., not based on response spectra). For example, [Penzien and Watabe \(1974\)](#) examined the principal axes of ground motions, that is, the orthogonal axes at which the components of ground accelerations are uncorrelated, of a sample consisting of only six ground motions recorded in six different earthquakes. From this very small sample of ground motions, they concluded that the major principal axis, which maximizes the Arias intensity ([Arias, 1970](#)), was oriented approximately towards the epicenter. [Kubo and Penzien \(1979\)](#) conducted a similar analysis in which they computed the principal axes of fifteen ground motions recorded during the 1971 M_w 6.6 San Fernando earthquake. They noted that, although the correlation was not strong, there was a tendency for the direction of the major principal axis or, in some cases, the intermediate principal axis to point in the direction of the slip zone, but noted that the correlation was not nearly as strong as previously reported by [Penzien and Watabe \(1974\)](#). However, this hypothesis of major principal axes oriented towards the epicenter, which was based on very limited data, appears not to be supported by more recent data (e.g., [Rezaeian and Der Kiureghian, 2012](#)).

[Bonamassa and Vidale \(1991\)](#) studied bandpass filtered particle motions from 10 aftershocks of the 1989 M_w 6.9 Loma Prieta earthquake, showing that for frequencies between 1 to 18 Hz several records presented orientations of polarization that were similar for most aftershocks, which they attributed to local site effects. [Vidale and Bonamassa \(1994\)](#) used bandpass filtered particle motions from the Loma Prieta mainshock to show that the orientations of ground shaking for frequencies lower than 1 Hz agrees with the orientations predicted from the focal mechanism. Similarly, [Borcherdt and Glassmoyer \(1992\)](#) found larger peak amplitudes in the transverse orientation than in the radial orientation for 27 of 34 ground motions recorded in the San Francisco Bay Area during the Loma Prieta mainshock but did not evaluate orientations of maximum spectral response.

Response spectra at distances of earthquake engineering interest are usually controlled by secondary, S, waves since they tend to produce the most intense ground shaking. Theoretical ground motion solutions within a homogeneous propagation medium from S-waves originating from a point shear dislocation have a deterministic polarization that is transverse to the direction of propagation ([Aki and Richards, 2002](#)), which suggests that the orientation of maximum horizontal response spectra at a site should be close to an orientation that is perpendicular to the line segment between the site and the epicenter (i.e., the transverse orientation). Although real earthquake sources, propagation mediums, and site effects are far more complex than this simplified theoretical case, it is interesting to investigate if the orientations of maximum horizontal response spectral ordinates are closer to the transverse orientation than would be expected if these orientations were fully random, especially for cases when some simplifying assumptions are closer to that of the theoretical case (e.g., at low frequencies).

This work examines the orientations that maximize response spectral ordinates using more than five thousand ground motion records from the NGA-West2 database ([Ancheta et al., 2014](#)). The orientations of maximum spectral response are compared with the transverse orientations predicted by the simplified theoretical S-wave polarization for several earthquake events. Contrary to pre-

vious works that have studied angular differences between the orientation of maximum spectral response and the strike-normal orientation, the latter being common for all recording stations, this work examines angular differences between the orientation of maximum spectral response and the transverse orientation, the latter being different for each recording station. The previous approach implicitly assumes that there is a predominant orientation common to all stations, whereas this study departs from this assumption and observes that the predominant orientation is controlled by the geographic location of each station relative to the seismic source. Finally, probability distributions are fitted for the angular difference between the orientation of maximum spectral response and the transverse orientation for different periods and styles of faulting.

Orientation of maximum spectral response

Earthquake ground motions are usually characterized for engineering purposes by response spectra, that is, by the peak (i.e., maximum absolute) response of linear elastic oscillators. Within the horizontal plane, the responses of the oscillators can be significantly polarized, especially at long periods. For example, Figure 1 shows relative displacement hodograms of 5%-damped oscillators of period 10 s subjected to horizontal ground motion components at each station within the Los Angeles Metropolitan Area recorded during the 1999 M_w 7.1 Hector Mine earthquake. The figure shows that the response of most oscillators to this earthquake occurs mainly in a specific orientation that is very similar for sites that are close to each other. As illustrated by Figure 2, which corresponds to the relative displacement hodogram for the Long Beach station, the orientation that maximizes the spectral response within the horizontal plane corresponds to the axis that passes through the resting position of the oscillator and the point within the hodogram that is farthest away from this resting position. This axis is also referred to as the major response axis or as the orientation of RotD100. In general, this orientation may change with the period of the oscillator and to a lesser extent also with its damping ratio, although for this work the latter was kept constant at the commonly used value of 5%.

Figure 3 shows the orientation of maximum spectral response using black line segments for 10-s oscillators during the same earthquake but now for a larger geographical region that includes the earthquake epicenter. As seen in the figure, for a majority of recording stations the orientation of maximum spectral response tends to occur close to the transverse orientation, which is depicted at each site by a gray line segment. We define the angular difference between these two orientations as $\alpha \in [-90^\circ, 90^\circ]$, and measured positive counterclockwise from the transverse orientation. The angular distance between the two orientations, $|\alpha|$, is represented by the color of the circle at each recording site. If all orientations of maximum spectral response were equally likely with respect to the transverse orientation, the mean value of $|\alpha|$ would be 45° . However, the value of $|\alpha|$ at most sites is significantly lower than 45° , with the mean value being 11.3° , again showing that, for this earthquake and period, the orientation of maximum spectral response tends to be close to the transverse orientation, which is actually perpendicular to the early observations by [Penzien and Watabe \(1974\)](#).

The same representation of Figure 3 is shown in Figure 4 but now for six significant earthquakes that affected the Los Angeles Metropolitan Area. In addition to the Hector Mine earthquake, Figure 4 also shows the orientation of maximum spectral response for the the 1992 M_w 7.3 Landers, 2008 M_w 5.4 Chino Hills, and 2010 M_w 7.2 El Mayor-Cucapah earthquakes, as well as the 2019 M_w 7.1

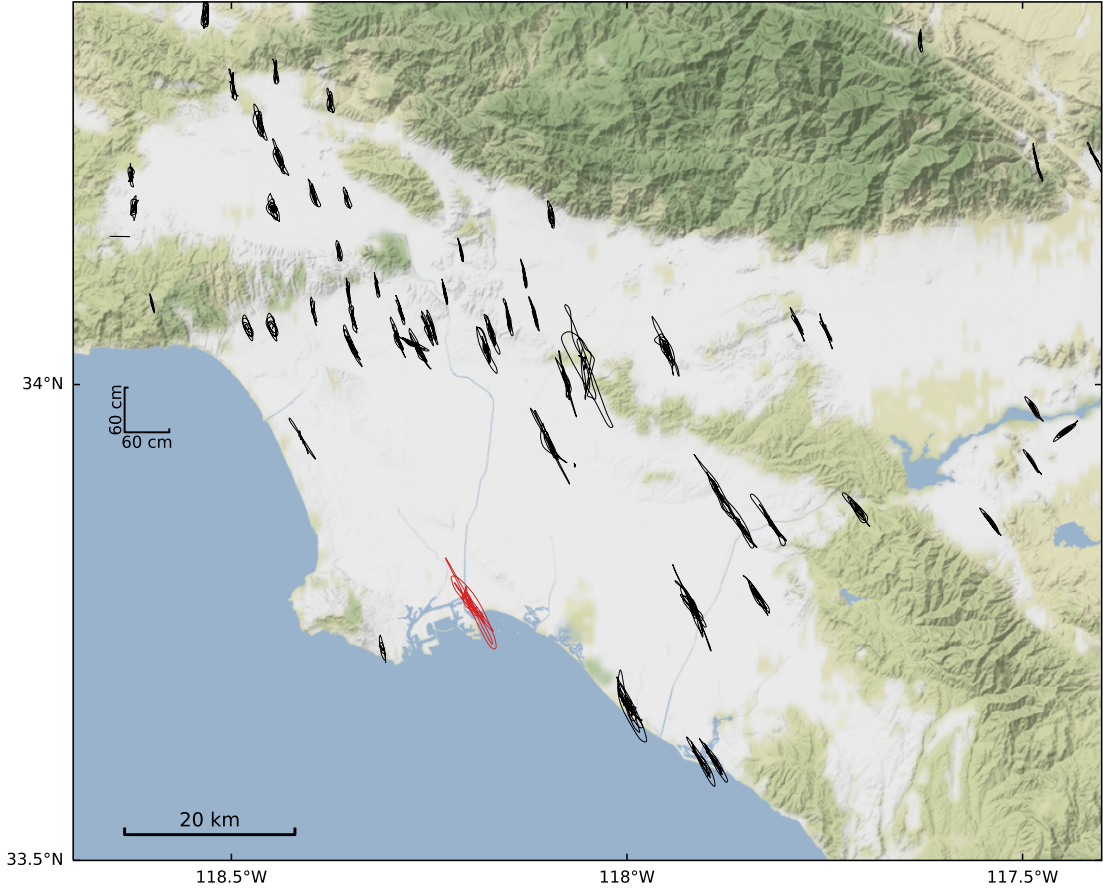


Figure 1: Relative displacement hodograms of 5%-damped linear elastic oscillators with periods of 10 s subjected to the horizontal components of ground motions recorded in the Los Angeles Metropolitan Area during the 1999 M_w 7.1 Hector Mine earthquake. The earthquake epicenter is outside the map limits to the east-northeast (see Figure 3). The hodogram in red is at the Long Beach station (see Figure 2).

and M_w 6.4 Ridgecrest earthquakes. Figure 4 also presents polar histograms with the orientations of maximum 10-s spectral response from all sites shown in each panel, which are grouped in bins of 10° and the lengths of the bars are proportional to the number of records that have their orientation of maximum spectral response within each 10° bin. All earthquakes presented in this figure have a predominant orientation within the Los Angeles Metropolitan Area. The mean value of $|\alpha|$ of the records in each earthquake is presented in the lower right corner of each panel. Every earthquake shown in Figure 4 has a mean $|\alpha|$ value that is significantly lower than 45° , showing that the orientations of maximum spectral response are, on average, fairly close to the transverse orientation. The title of each panel in Figure 4 also presents the rake angle, λ , of the corresponding earthquake, obtained from the Global Centroid Moment Tensor catalog (see Data and Resources Section), showing that the 2008 M_w 5.4 Chino Hills earthquake has oblique faulting and the other five earthquakes have strike-slip faulting.

Figure 5 shows the orientations of maximum spectral response at 10 s of ground motions from nine shallow crustal earthquakes in different parts of the world. These orientations are presented

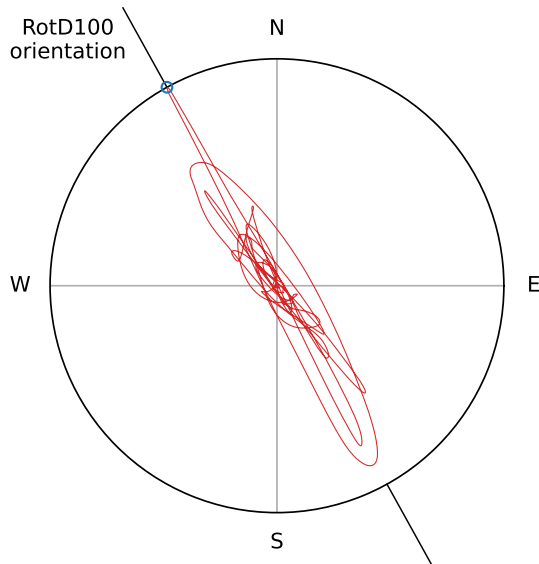


Figure 2: Relative displacement hodogram of a 5%-damped linear elastic oscillator with a period of 10 s subjected to both horizontal components of ground motions recorded at the Long Beach station during the 1999 M_w 7.1 Hector Mine earthquake.

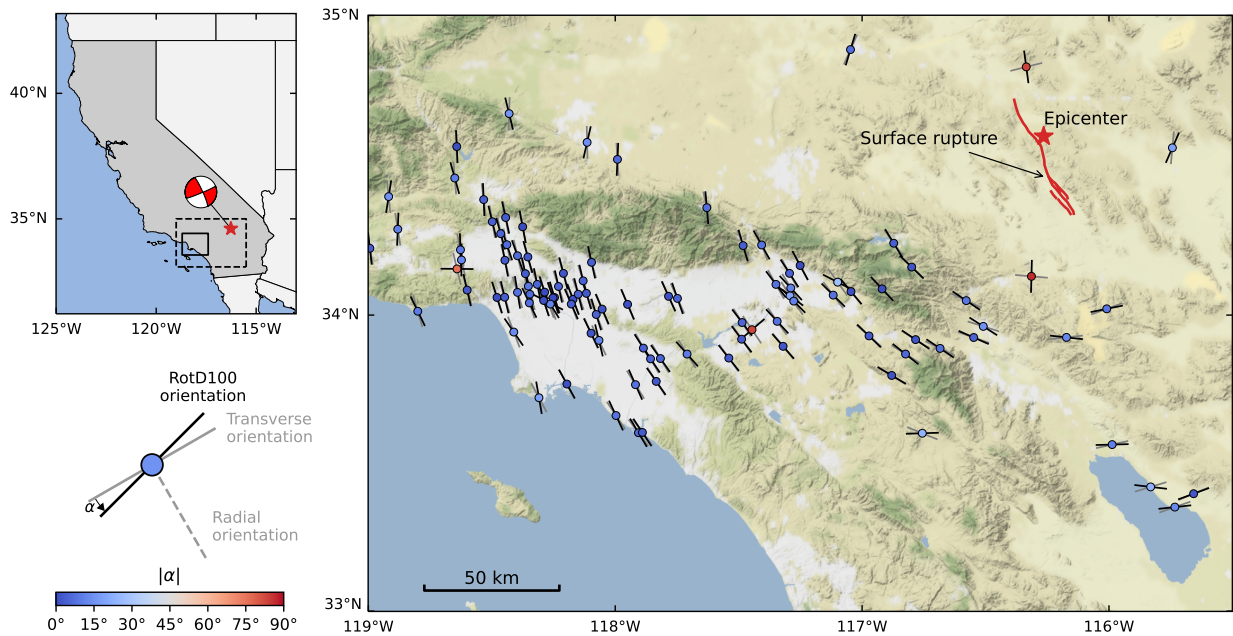


Figure 3: Orientations of maximum spectral response for oscillators with periods of 10 s subjected to the horizontal components of ground motions recorded during the 1999 M_w 7.1 Hector Mine earthquake. The surface rupture was obtained from [Treiman et al. \(2002\)](#). The upper left map shows the location of the main map (dashed black rectangle) and the maps of Figure 4 (solid black rectangle) within California.

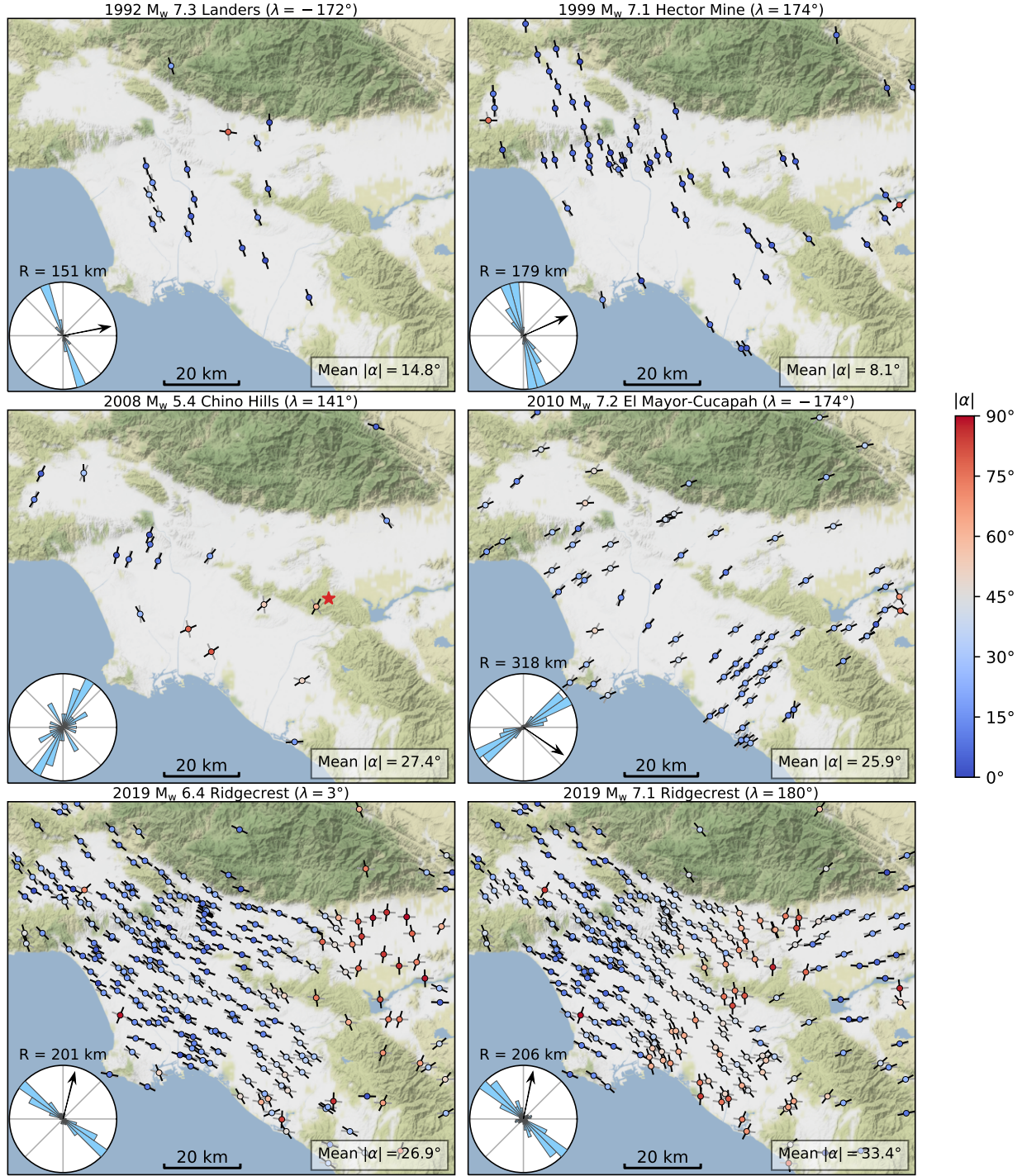


Figure 4: Orientation of maximum spectral response for oscillators with periods of 10 s subjected to the horizontal components of ground motions recorded in the Los Angeles Metropolitan Area during six earthquakes. The polar histogram within each panel represents the number of stations with maximum spectral response within bins of 10° . The black arrow within each histogram represents the direction from the center of the map to the earthquake epicenter. The distances from the center of the map to each earthquake epicenter (R) are presented above the corresponding histograms.

using black lines and can be compared to the transverse orientation represented by the gray concentric circles centered at the earthquake epicenter. Mean $|\alpha|$ values for each earthquake are again presented in each panel, but now considering all usable records of each earthquake. For the 1999 M_w 7.1 Hector Mine earthquake and the 2010 M_w 7.2 El Mayor-Cucapah earthquake, please note that the mean values differ from those previously shown in Figure 4 because they were only for stations within the Los Angeles Metropolitan Area, whereas those in Figure 5 were computed using more stations covering a much larger geographical region. The rake angle of each earthquake is again indicated in parenthesis in the title of each panel. It can be seen that most earthquakes with reverse faulting have mean $|\alpha|$ values relatively close to 45° , except for the 2008 M_w 6.9 Iwate earthquake. Conversely, all strike-slip earthquakes presented in Figure 5, which include the 1999 M_w 7.1 Hector Mine, 2002 M_w 6.7 Nenana Mountain, 2010 M_w 7.2 El Mayor-Cucapah, and 2010 M_w 7.1 Darfield earthquakes, as well as a M_w 6.4 aftershock of the 1999 Chi-Chi earthquake, have mean $|\alpha|$ values much lower than 45° , indicating that the orientation of maximum spectral response tends to occur close to the transverse orientation. Records from the 1994 M_w 6.7 Northridge earthquake were also analyzed; however, they were not included in Figures 4 and 5 because only one record had a maximum usable period greater than or equal to 10 s. If records from this earthquake were to be used regardless of their maximum usable period, there would be 142 records and their mean $|\alpha|$ value would be 46.3° , again close to 45° as with most other earthquakes with reverse faulting that were studied.

Statistical characterization of α

To obtain results that are more statistically significant, the angular differences between maximum spectral response and transverse orientations were computed at periods between 0.01 to 10 s for 5065 ground motion records, which correspond to all the records within the NGA-West2 ground motion database ([Ancheta et al., 2014](#)) that were recorded during earthquakes of magnitude greater than or equal to 5.0; at stations with NEHRP site classes B, C, and D; and that reasonably represent free-field conditions (according to the criteria used by [Boore et al., 2014](#)). Moreover, the records were only used to compute response spectra up to their maximum usable period, which is defined by the NGA-West2 database, resulting in a decreasing number of usable records as the period increases. These same filters were used for the ground motions presented in all figures within this document. The ground motions were grouped by their style of faulting, which was defined based on the rake angle reported within the NGA-West2 database. Reverse earthquakes were assumed to have rake angles, λ , within $[60^\circ, 120^\circ]$ and strike-slip earthquakes were assumed to have rake angles that are within 30° of a horizontal slip vector (i.e., $\lambda = 0^\circ$, $\lambda = 180^\circ$, or $\lambda = -180^\circ$). Records from oblique and normal earthquakes were not considered for these statistics due to their relatively low number in the database.

Figure 6 shows the mean angular distance between the orientation of maximum spectral response and the transverse orientation, $|\alpha|$, as a function of period. The mean values were computed separately for records from reverse and strike-slip earthquakes. If all orientations of maximum spectral response were equally likely with respect to the transverse orientation, the mean value of $|\alpha|$ would be 45° , which is actually very close to the results obtained at all periods for records from reverse-faulting earthquakes, indicating that the orientation of maximum spectral response for reverse faulting earthquakes has no clear trend with respect to the location of the epicenter.

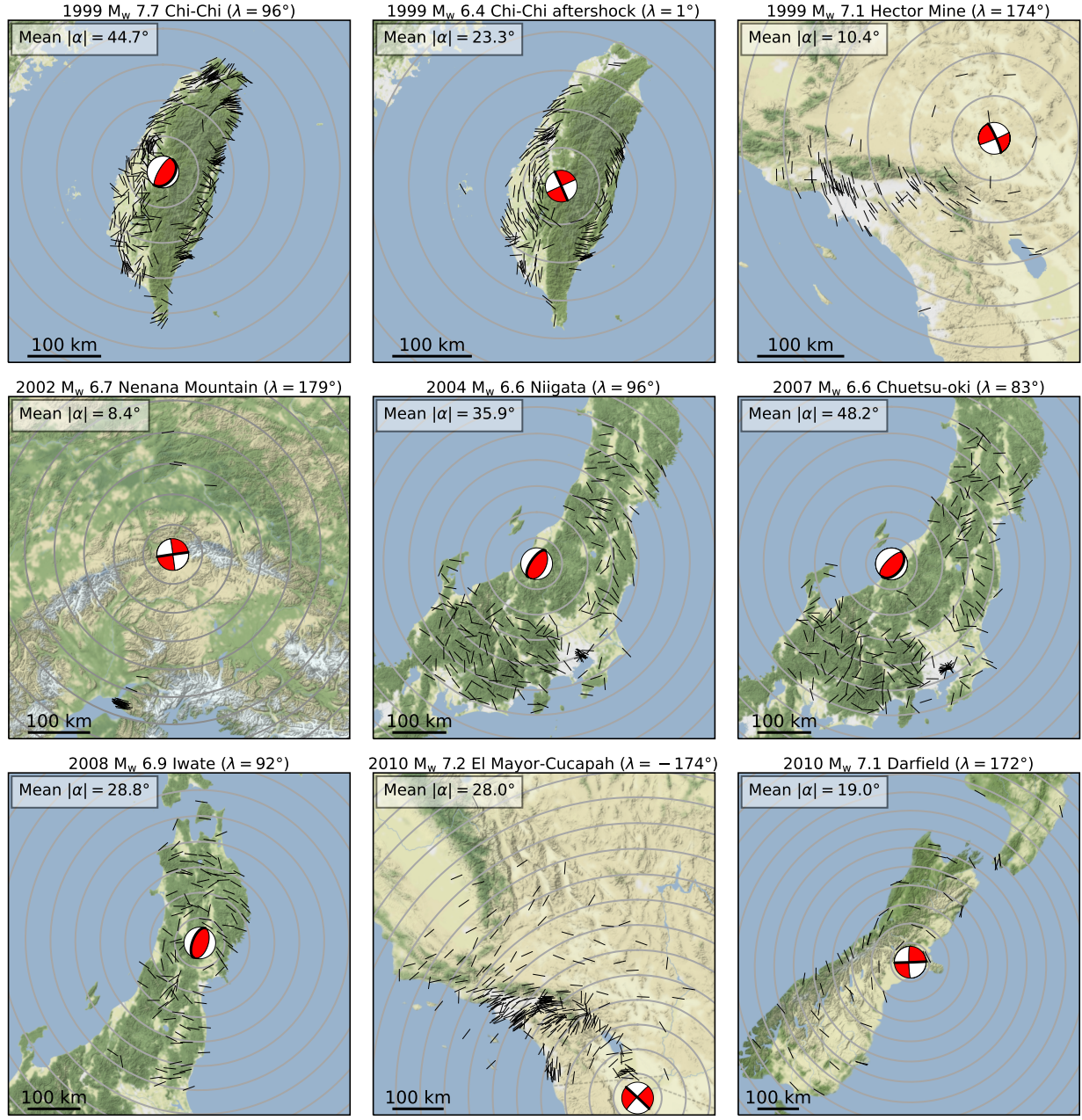


Figure 5: Orientation of maximum spectral response for oscillators with periods of 10 s subjected to the horizontal components of ground motions of nine shallow crustal earthquakes. The gray concentric circles are used to indicate the transverse orientation every 50 km from the epicenter. Thicker black lines in the focal mechanisms indicate the preferred fault planes.

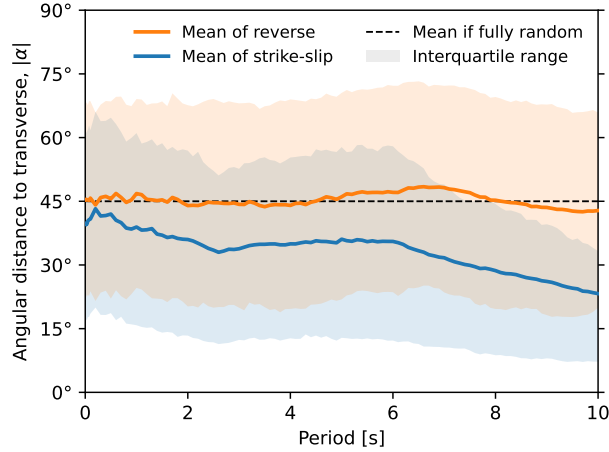


Figure 6: Mean angular distance between the transverse orientation and the orientation of maximum spectral response as a function of period for reverse and strike-slip earthquakes. Shaded areas indicate interquartile ranges and the dashed black line is the expected mean angular distance if the orientations of maximum spectral response were equally likely with respect to the transverse orientation (i.e., 45°)

However, records with strike-slip faulting have mean values of $|\alpha|$ that are significantly lower than 45° and that decrease as the period becomes longer. Thus, the orientations of maximum spectral response become closer to the transverse orientation. This is possibly due to the fact that, for strike-slip earthquakes, the dominant shear waves tend to be SH waves whose motion is horizontal and perpendicular to the propagation directions, that is, in the transverse orientation. Furthermore, as shown in Figure 6, the mean angular distance decreases as the period increases, meaning that the orientation of maximum spectral response becomes closer to the transverse orientation as period increases. This is because the peak relative displacement of the oscillators become increasingly correlated to peak ground displacements as the oscillator period increases.

The values of angle α from all records with strike-slip faulting were used to fit an axial normal distribution (Arnold and SenGupta, 2006), which can be derived from the von Mises distribution (also known as the circular normal distribution). If Φ is a random variable with a von Mises distribution, its probability density function is:

$$f_{\Phi}(\phi; \mu, \tau) = \frac{e^{\tau \cos(\phi - \mu)}}{2\pi I_0(\tau)}, \quad \phi \in [-\pi, \pi] \quad (1)$$

where μ and τ are the parameters of the distribution; $I_0(\tau)$ is the modified Bessel function of order 0; and ϕ is a realization of random variable Φ . Although parameter τ of the von Mises probability distribution is usually denoted by κ in the literature, herein the notation was changed to avoid confusion with the spectral decay parameter (Anderson and Hough, 1984). The von Mises distribution is commonly used when dealing with angular data that have a periodicity of 360° because it is the maximum entropy distribution for a fixed circular mean and circular variance. However, spectral responses within the horizontal plane have a periodicity of 180° because of the absolute value used in their computation, and hence the orientation of their maximum also has the same periodicity. The probability density function of this type of variable, A , with periodicity of

180° can be found by adding the probability density functions of random variables with periodicity of 360° but from angles that are separated by 180° as follows:

$$f_A(\alpha; \mu, \tau) = f_\Phi(\alpha; \mu, \tau) + f_\Phi(\alpha + \pi; \mu, \tau) \quad (2)$$

$$= \frac{\cosh(\tau \cos(\alpha - \mu))}{\pi I_0(\tau)}, \quad \alpha \in [-\pi/2, \pi/2] \quad (3)$$

where α is a realization of the random variable A with periodicity 180° . Furthermore, assuming that the mean of the distribution is zero (i.e., $\mu = 0$), which means that there is no preference for angles to be clockwise or counterclockwise away from the transverse orientation, leads to a probability distribution defined by a single parameter τ given by:

$$f_A(\alpha; \tau) = \frac{\cosh(\tau \cos(\alpha))}{\pi I_0(\tau)}, \quad \alpha \in [-\pi/2, \pi/2] \quad (4)$$

Parameter τ was fitted for each period using a maximum likelihood estimation:

$$\hat{\tau} = \arg \max_{\tau \in [0, \infty)} \prod_{i=1}^n f_A(\alpha_i; \tau) \quad (5)$$

$$= \arg \max_{\tau \in [0, \infty)} \sum_{i=1}^n \log(\cosh(\tau \cos(\alpha_i))) - n \log(I_0(\tau)) \quad (6)$$

where α_i is the angular difference between the orientation of maximum spectral response and the transverse orientation for the i -th ground motion. Separate probability distributions of α were fitted for records from strike-slip and reverse earthquakes.

Figure 7 shows the fitted probability distributions of α corresponding to periods of 0.1, 4, and 10 s for strike-slip earthquakes, together with the empirical distributions from the data. For these types of earthquakes, the value of τ increases as the period gets longer, which leads to larger probability densities around the transverse orientation ($\alpha = 0^\circ$) and lower mean values of $|\alpha|$. On the other hand, equivalent distributions for records from reverse earthquakes are presented in Figure 8, showing that the distribution of α is relatively close to a uniform probability distribution (i.e., characterized by low values of τ), again suggesting that there is no predominance of the orientation of maximum spectral response to occur at or near the transverse orientations for earthquake with this style of faulting.

Distributions of α were fitted separately for 105 periods between 0.01 and 10 s, resulting in the values of τ shown in Figure 9. The results again show that for strike-slip earthquakes, τ tends to increase as the period becomes longer, leading to a higher likelihood of the orientation of maximum spectral response being close to the transverse orientation. For reverse earthquakes, τ is zero for all periods lower than 9.5 s, which corresponds to a uniform probability distribution. For periods between 9.5 and 10 s, τ is approximately 0.7, although for practical applications it may be reasonable to just assume a uniform distribution at all periods.

Discussion

Several previous studies have assumed explicitly or implicitly that the orientation of maximum spectral response occurs close to the strike-normal orientation (e.g., [Somerville et al., 1997](#)). This

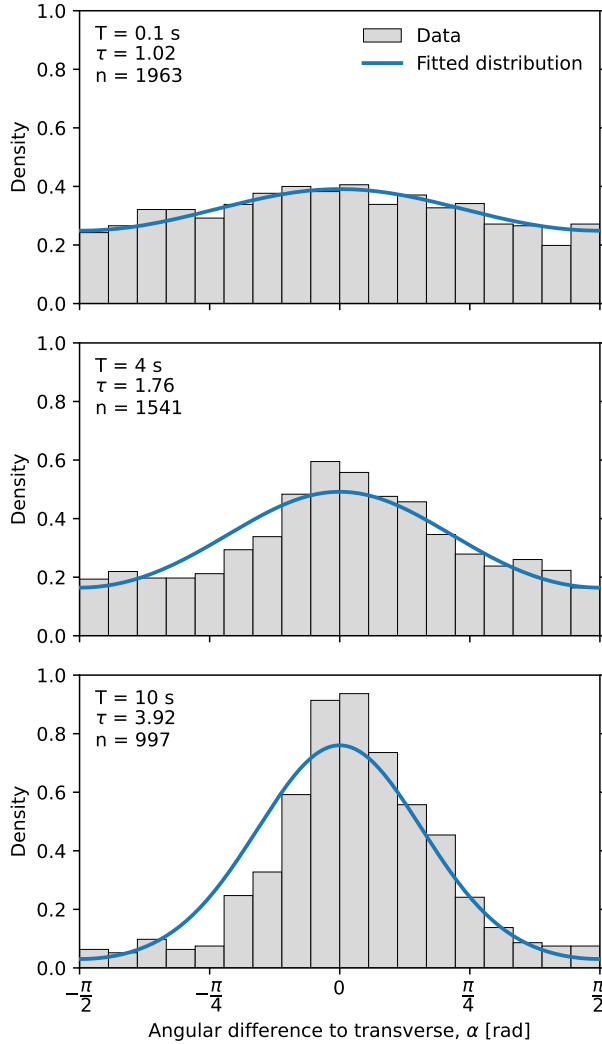


Figure 7: Empirical and fitted distributions of the angular differences between the transverse orientation and the orientations of maximum spectral response at periods of (a) 0.1 s, (b) 4 s, and (c) 10 s for record from strike-slip earthquakes. The period (T), fitted parameter of the distribution (τ), and number of records used for each case (n) are presented within each panel.

has led previous works to study the angle between the orientation of maximum spectral response and the strike-normal orientation (e.g., [Shahi and Baker, 2014](#)), which is a common orientation for all stations that recorded a given earthquake. To compare this previous assumption with the assumption of the transverse orientation identified in this study, which changes from station to station, Figure 10 shows distributions of angular differences between the orientations of maximum spectral response and the strike-normal orientations for strike-slip earthquakes (i.e., the same records used in Figure 7). Additionally, Figure 11 shows the angular differences for records at rupture distances shorter than 20 km. As expected, the distribution of angular differences in both cases is fairly uniform at 0.1 s because directionality effects are weak at high frequencies. For rupture distances shorter than 20 km, the maximum spectral responses at 4 and 7 s tend to be close to the strike-normal orientation for many of the records. However, as shown in Figure 11, the

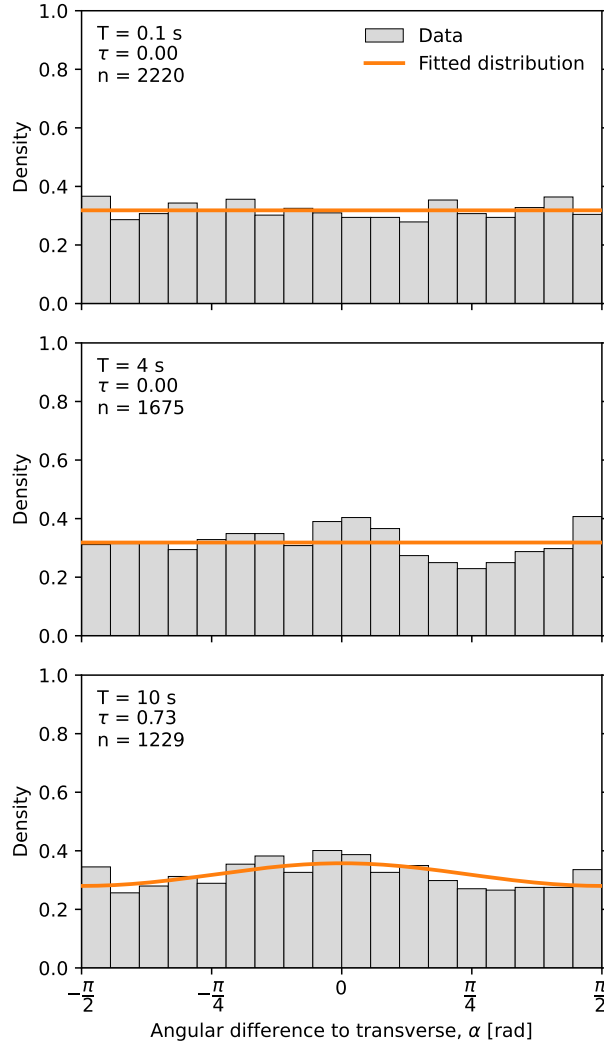


Figure 8: Empirical and fitted distributions of the angular differences between the transverse orientation and the orientations of maximum spectral response at periods of (a) 0.1 s, (b) 4 s, and (c) 10 s for records from reverse earthquakes. The period (T), fitted parameter of the distribution (τ), and number of records used for each case (n) are presented within each panel.

distributions become fairly uniform after removing records with rupture distances shorter than 5 km, suggesting that the strike-normal orientation is more predominant within this shorter distance range. Although this trend could be somewhat affected by the low number of records available at these short distances, the data supports considering strike-normal motions in the near-fault region of strike-slip earthquakes. However, when looking at all distances (Figure 10), the distribution is close to uniform at 4 s and seems to favor the strike-parallel orientation at 10 s, although this may be because, for 10 s, the locations of the recording stations with respect to the strikes lead to the strike-normal orientation being further away from the transverse orientation than expected, with an average angular distance between the strike-normal orientation and the transverse orientation of 54° , which is notably higher than the 45° that would be expected from fully random locations (see Figure S1, available in the supplemental material to this article). Thus, the orientations of

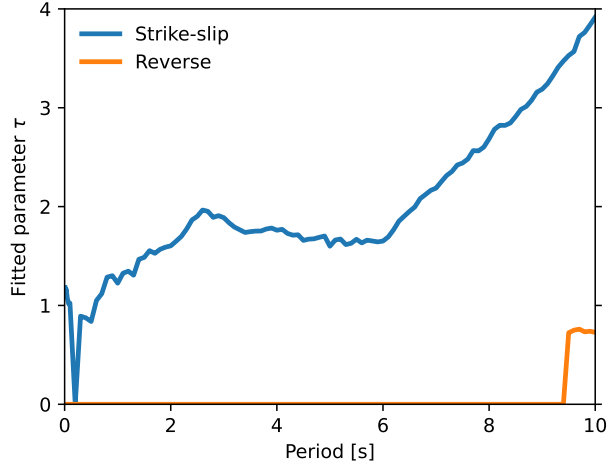


Figure 9: Values of parameter τ from the probability distributions of α fitted using records from strike-slip and reverse earthquakes.

maximum spectral response do not occur close to the strike-normal orientation when looking at all distances. On the other hand, as shown in Figure 7, the orientations of maximum spectral response are relatively close to the transverse orientations when looking at the same set of ground motion records. Establishing the limiting distances and transition between these two preferential orientations (i.e., strike-normal and transverse) requires further study.

[Shahi and Baker \(2014\)](#) found that the orientation of maximum spectral response is only close to the strike-normal orientation for rupture distances shorter than 5 km. However, [Bradley and Baker \(2015\)](#) noticed that during the 2010 M_w 7.0 Darfield earthquake, there were 19 recording stations where the orientation of maximum intensity occurred close to the strike-normal orientation at distances as large as 30 km, in apparent contradiction with previous observations by [Shahi and Baker \(2014\)](#). To study this apparent inconsistency in light of the observations in the present study, we evaluated the position of these 19 recording stations relative to the epicenter and the strike of the fault. As seen in Figure 12, all 19 stations studied by [Bradley and Baker \(2015\)](#) were located to the east of the earthquake rupture and the fault strike was approximately in the east-west orientation, hence the transverse orientations at all stations were very close to the strike-normal orientation. The average angular difference between the strike-normal orientation and the transverse orientation of these stations was only 7.0° and the maximum angular difference of all station was 22.9° . Figure 12 also shows that other ground motions from the NGA-West2 database that were not considered by [Bradley and Baker \(2015\)](#) and were recorded outside of the Christchurch urban area at similar distances have orientations of maximum spectral response at 10 s that are closer to the transverse orientation than to the strike-normal orientation. Moreover, Figure 5 shows that using ground motions from this same earthquake recorded at a broader range of locations leads to orientations of maximum spectral response that are close to the transverse orientation, with an average angular distance to the transverse orientation of 19° for 10 s. Thus, the reason for observing orientations of maximum spectral response close to the strike-normal orientation for rupture distances up to 30 km in those 19 stations was probably that all included stations are within the Christchurch urban area, which all had very similar locations relative to the earthquake source. Thus, the orientation of maximum spectral response would not be expected to be close to the strike-normal orientation

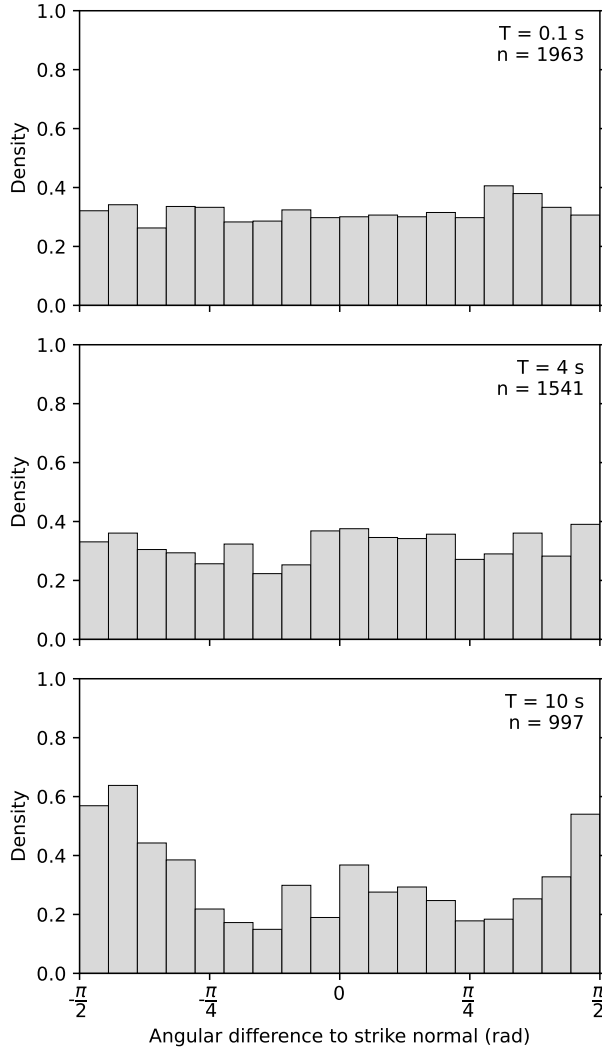


Figure 10: Empirical distributions of the angular differences between the orientation of maximum spectral response and the strike-normal orientation for records from strike-slip earthquakes. The period (T) and number of records used for each case (n) are presented within each panel.

at distances of up to 30 km in a general case.

Motivated by theoretical point sources, this study uses earthquake epicenter to define transverse orientations. However, this assumption has several limitations, especially for sites located in the very near field of large-magnitude earthquakes. Ground motions are a combination of waves originating from different locations of the rupture surface. Thus, if the source-to-site distance is short relative to the rupture length, the transverse orientation could change significantly depending on the location of the rupture where larger amplitude waves originate from. Moreover, large-magnitude earthquakes may also have their largest slip at a location that is relatively far away from the hypocenter, which was the case, for example, for the 2002 M_w 7.9 Denali earthquake. Despite these limitations, this work shows that the simple epicenter assumption has a significant capacity to predict orientations of maximum spectral response, which may be attributed to the fact that, for large-magnitude strike-slip earthquakes, the hypocenter is usually very close to large-slip asperities

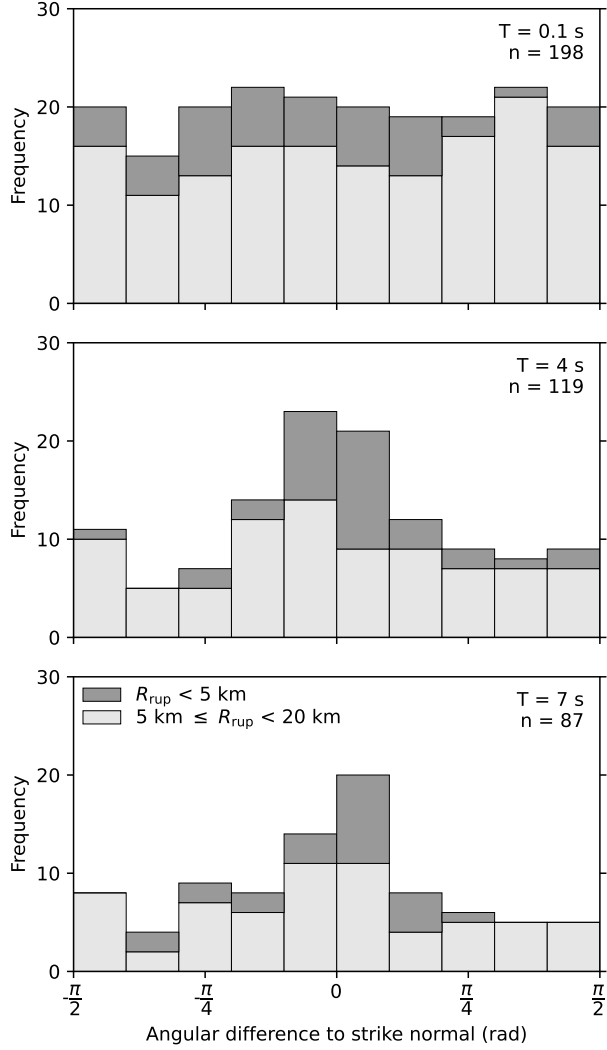


Figure 11: Empirical distributions of the angular differences between the strike-normal orientation and the orientations of maximum spectral response at periods of (a) 0.1 s, (b) 4 s, and (c) 10 s for records from strike-slip earthquakes with rupture distances shorter than 20 km. The period (T) and number of records used for each case (n) are presented within each panel.

(Mai et al., 2005). However, better predictions of the orientation of maximum spectral response in the very near field can probably be achieved by considering a more complete characterization of the spatial and temporal distribution of the slip within the rupture. Nevertheless, one must consider the often significant discrepancies in the inferred slip distributions between different models depending on several assumptions, such as the stations selected in the inversion, differences in data processing and weighting, and choice of inversion method. Furthermore, the number of records available in the very near field of large-magnitude strike-slip earthquakes is, at present time, very limited.

S waves from theoretical double couple point sources within a homogeneous propagation medium have far-field radiation patterns and polarizations that are deterministic (Aki and Richards, 2002), which motivated this study. The result that the orientation of maximum spectral response of

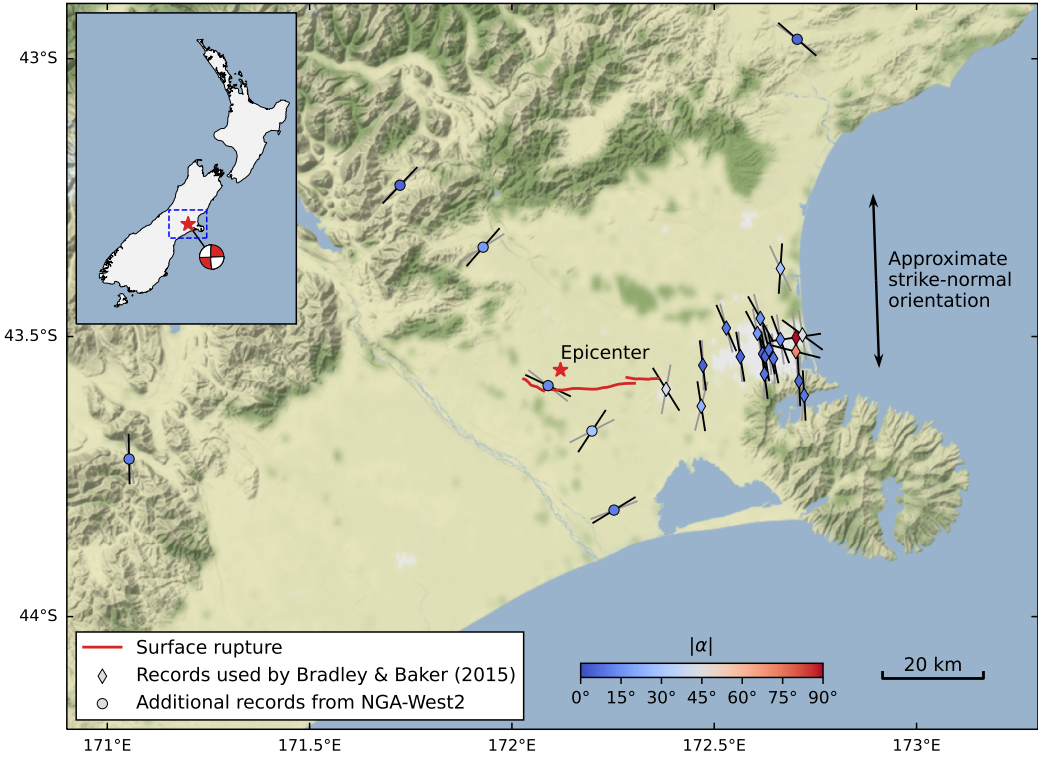


Figure 12: Orientations of maximum spectral response for oscillators with periods of 10 s subjected to the horizontal components of ground motions recorded during the 2010 M_w 7.1 Darfield earthquake. Five of the records used by Bradley and Baker (2015) have maximum usable periods shorter than 10 s, but are still shown here for comparison purposes. The surface rupture was obtained from Quigley et al. (2012). The offset of the epicenter from the fault trace has been attributed to the rupture starting within a smaller reverse fault that then triggered the rupture on the main Greendale fault (Gledhill et al., 2011; Beavan et al., 2012). The upper left inset shows the location of the map (blue rectangle) within New Zealand.

records from strike-slip earthquakes is usually close to the transverse orientation can therefore be explained by comparing the radiation patterns of SH and SV waves, which in the horizontal plane are polarized in the transverse and radial orientations, respectively. Indeed, vertical strike-slip sources usually have SH radiation patterns that are much more intense than SV radiation patterns. On the other hand, SH and SV radiation patterns from reverse earthquakes have intensities that are much more comparable, with both patterns varying significantly with the specific rake, dip, and takeoff angle (Aki and Richards, 2002). This could explain the apparent uniform distribution of the orientation of maximum spectral response relative to the transverse orientation for records from earthquakes with reverse faulting. Instead of having a binary model for records from strike-slip and reverse earthquakes, future works could probably find better estimates of the orientation of maximum spectral response by considering the specific theoretical radiation pattern of each earthquake, which would depend on fault mechanism, depth, takeoff angle, and source-receiver azimuth.

Another aspect to consider is that at sites far away from the seismic source and for long periods, spectral responses may be strongly influenced by surface waves instead of body waves. Neverthe-

less, the results of this study show that the orientations of maximum spectral response for records from strike-slip earthquakes are still close to the transverse orientation even at distances where surface waves may control. This may also at least partially be explained by the fact that radiation patterns of Love and Rayleigh waves are polarized in the transverse and radial orientations, respectively. For example, the radiation patterns developed by [Rösler and van der Lee \(2020\)](#) show that, for vertical strike-slip earthquakes, the intensity of Love waves is significantly larger than that of Rayleigh waves. Meanwhile, for reverse earthquakes, the radiation patterns of Love and Rayleigh waves are closer in terms of intensity and vary widely depending on the specific fault mechanism and depth ([Rösler and van der Lee, 2020](#)), which could explain the approximately uniform distribution of the orientation of maximum spectral response relative to the transverse orientations when combining records from all earthquakes with reverse faulting.

Conclusions

This work studied the orientation in which the maximum response spectral ordinate occurs within the horizontal plane using a database of 5065 ground motion records from shallow crustal earthquakes in active tectonic regions. For strike-slip earthquakes, these orientations were found to occur much closer to the transverse orientation than would be expected if they were random (i.e., with uniformly distributed orientations). These orientations also become closer to the transverse orientation as the period increases, with, for example, mean angular differences between these orientations being 36° and 23° for periods of 2 and 10 s, respectively. On the other hand, ground motions from reverse earthquakes were found to show no particular trend in the orientation of maximum spectral response relative to the transverse orientation, with mean differences to the transverse orientation very close to 45° for all studied periods. These results are consistent with some of those found by [Kotha et al. \(2019\)](#) while studying radiation patterns of average horizontal response spectra, where the anisotropic radiation pattern of theoretical S-waves was much closer to empirical radiation patterns in strike-slip earthquakes than in reverse earthquakes.

Probability distributions of the angle between the orientation of maximum spectral response and the transverse orientation were fitted for strike-slip earthquakes at different structural periods. The fitted probability distributions are fully-defined by a single period-dependent parameter that describes the tendency of the orientation of maximum spectral response to be closer to the transverse orientation. Given an earthquake epicenter, these distributions can be used to sample the orientation of maximum spectral response of future strike-slip earthquakes. Moreover, the fitted period-dependent distributions can be used together with a GMM and a probabilistic model of directionality (e.g., [Poulos and Miranda, 2022](#)) to compute response spectra at fixed orientations of interest within a site, such as the orientations of the principal response axes of a building. A more direct model could be developed in the future to transform the intensity provided by a GMM (usually RotD50) to an intensity in the orientations of interest, and hence not requiring the sampling of the orientation of maximum spectral response. To use these models within a probabilistic seismic hazard analysis (PSHA), the epicentral location needs to be randomized within each strike-slip fault, which is already considered by most PSHA calculations.

A better estimate of the orientation of maximum horizontal response spectra can probably be found by considering the specific characteristics of each record, such as its source, path, and site properties, which could be achieved by, for example, using physics-based simulations. However,

the simplicity of the presented empirical model makes it compelling for practical applications, especially for cases when these types of analyses cannot be performed due to computational limitations or lack of input data.

Data and Resources

The ground motion records from the 2019 M_w 7.1 and M_w 6.4 Ridgecrest earthquakes, which were only used in Figure 4, were obtained from the Center for Engineering Strong Motion Data (<https://strongmotioncenter.org/>, last accessed March 2022). The networks or agencies that provided this data were the California Strong Motion Instrumentation Program (CSMIP), the Southern California Seismic Network (SCSN, doi:[10.7914/SN/CI](https://doi.org/10.7914/SN/CI)), and the USGS National Strong Motion Project (NSMP, doi:[10.7914/SN/NP](https://doi.org/10.7914/SN/NP)). All other ground motion records used in this study were obtained from the NGA-West2 ground motion database developed by the Pacific Earthquake Engineering Research Center (<https://ngawest2.berkeley.edu/spectras/new>, last accessed April 2020). Focal mechanisms were obtained from the Global Centroid Moment Tensor catalog using <https://www.globalcmt.org/CMTsearch.html> (last accessed December 2022). Map figures used tiles by Stamen Design, under CC BY 3.0, and basemap data by OpenStreetMap, under ODbL. The supplemental material provides a figure with histograms of the angular distances between transverse and strike-normal orientations.

Acknowledgments

The authors would like to acknowledge the National Agency for Research and Development (ANID) / Doctorado Becas Chile / 2019-72200307 and the Nancy Grant Chamberlain Fellowship at Stanford University for sponsoring the doctoral studies of the first author. The authors would also like to thank the insightful comments and suggestions of Julian Bommer, Kyle Withers, and William Ellsworth. The authors are also grateful to the Pacific Earthquake Engineering Research Center, the Center for Engineering Strong Motion Data, and the corresponding networks and agencies for gathering, processing, and distributing the ground motion records used in this study.

References

- Aki, K. and P. G. Richards (2002). *Quantitative seismology* (2nd ed.). University Science Books, Sausalito, CA.
- Ancheta, T. D., R. B. Darragh, J. P. Stewart, E. Seyhan, W. J. Silva, B. S.-J. Chiou, K. E. Wood-dell, R. W. Graves, A. R. Kottke, D. M. Boore, T. Kishida, and J. L. Donahue (2014). NGA-West2 database, *Earthquake Spectra* **30**, 989–1005.
- Anderson, J. G. and S. E. Hough (1984). A model for the shape of the Fourier amplitude spectrum of acceleration at high frequencies, *Bulletin of the Seismological Society of America* **74**, 1969–1993.

- Arias, A. (1970). A measure of earthquake intensity. In R. J. Hansen (Ed.), *Seismic Design for Nuclear Power Plants*, 438–483. MIT Press, Cambridge, MA.
- Arnold, B. C. and A. SenGupta (2006). Probability distributions and statistical inference for axial data, *Environmental and Ecological Statistics* **13**, 271–285.
- Beavan, J., M. Motagh, E. J. Fielding, N. Donnelly, and D. Collett (2012). Fault slip models of the 2010–2011 Canterbury, New Zealand, earthquakes from geodetic data and observations of postseismic ground deformation, *New Zealand Journal of Geology and Geophysics* **55**, 207–221.
- Beyer, K. and J. J. Bommer (2006). Relationships between median values and between aleatory variabilities for different definitions of the horizontal component of motion, *Bulletin of the Seismological Society of America* **96**, 1512–1522.
- Bonamassa, O. and J. E. Vidale (1991). Directional site resonances observed from aftershocks of the 18 October 1989 Loma Prieta earthquake, *Bulletin of the Seismological Society of America* **81**, 1945–1957.
- Boore, D. M. (2010). Orientation-independent, nongeometric-mean measures of seismic intensity from two horizontal components of motion, *Bulletin of the Seismological Society of America* **100**, 1830–1835.
- Boore, D. M. and T. Kishida (2017). Relations between some horizontal-component ground-motion intensity measures used in practice, *Bulletin of the Seismological Society of America* **107**, 334–343.
- Boore, D. M., J. P. Stewart, E. Seyhan, and G. M. Atkinson (2014). NGA-West2 equations for predicting PGA, PGV, and 5% damped PSA for shallow crustal earthquakes, *Earthquake Spectra* **30**, 1057–1085.
- Borcherdt, R. D. and G. Glassmoyer (1992). On the characteristics of local geology and their influence on ground motions generated by the Loma Prieta earthquake in the San Francisco Bay region, California, *Bulletin of the Seismological Society of America* **82**, 603–641.
- Bradley, B. A. and J. W. Baker (2015). Ground motion directionality in the 2010–2011 Canterbury earthquakes, *Earthquake Engineering & Structural Dynamics* **44**, 371–384.
- Campbell, K. W. and Y. Bozorgnia (2008). NGA ground motion model for the geometric mean horizontal component of PGA, PGV, PGD and 5% damped linear elastic response spectra for periods ranging from 0.01 to 10 s, *Earthquake Spectra* **24**, 139–171.
- Gledhill, K., J. Ristau, M. Reyners, B. Fry, and C. Holden (2011). The Darfield (Canterbury, New Zealand) Mw 7.1 earthquake of September 2010: a preliminary seismological report, *Seismological Research Letters* **82**, 378–386.
- Housner, G. W. (1952). Spectrum intensities of strong-motion earthquakes. In *Proceedings of the Symposium on Earthquake and Blast Effects on Structures*, Los Angeles, CA, 20–36. Earthquake Engineering Research Institute.

- Howard, J. K., C. A. Tracy, and R. G. Burns (2005). Comparing observed and predicted directivity in near-source ground motion, *Earthquake Spectra* **21**, 1063–1092.
- Huang, Y.-N., A. S. Whittaker, and N. Luco (2008). Maximum spectral demands in the near-fault region, *Earthquake Spectra* **24**, 319–341.
- Kotha, S. R., F. Cotton, and D. Bindi (2019). Empirical models of shear-wave radiation pattern derived from large datasets of ground-shaking observations, *Scientific Reports* **9**, 1–11.
- Kubo, T. and J. Penzien (1979). Analysis of three-dimensional strong ground motions along principal axes, San Fernando earthquake, *Earthquake Engineering & Structural Dynamics* **7**, 265–278.
- Mai, P. M., P. Spudich, and J. Boatwright (2005). Hypocenter locations in finite-source rupture models, *Bulletin of the Seismological Society of America* **95**, 965–980.
- Penzien, J. and M. Watabe (1974). Characteristics of 3-dimensional earthquake ground motions, *Earthquake Engineering & Structural Dynamics* **3**, 365–373.
- Poulos, A. and E. Miranda (2022). Probabilistic characterization of the directionality of horizontal earthquake response spectra, *Earthquake Engineering & Structural Dynamics* **51**, 2077–2090.
- Quigley, M., R. Van Dissen, N. Litchfield, P. Villamor, B. Duffy, D. Barrell, K. Furlong, T. Stahl, E. Bilderback, and D. Noble (2012). Surface rupture during the 2010 Mw 7.1 Darfield (Canterbury) earthquake: Implications for fault rupture dynamics and seismic-hazard analysis, *Geology* **40**, 55–58.
- Rezaeian, S. and A. Der Kiureghian (2012). Simulation of orthogonal horizontal ground motion components for specified earthquake and site characteristics, *Earthquake Engineering & Structural Dynamics* **41**, 335–353.
- Rösler, B. and S. van der Lee (2020). Using seismic source parameters to model frequency-dependent surface-wave radiation patterns, *Seismological Research Letters* **91**, 992–1002.
- Shahi, S. K. and J. W. Baker (2014). NGA-West2 models for ground motion directionality, *Earthquake Spectra* **30**, 1285–1300.
- Somerville, P. G. (2003). Magnitude scaling of the near fault rupture directivity pulse, *Physics of the Earth and Planetary Interiors* **137**, 201–212.
- Somerville, P. G., N. F. Smith, R. W. Graves, and N. A. Abrahamson (1997). Modification of empirical strong ground motion attenuation relations to include the amplitude and duration effects of rupture directivity, *Seismological Research Letters* **68**, 199–222.
- Treiman, J. A., K. J. Kendrick, W. A. Bryant, T. K. Rockwell, and S. F. McGill (2002). Primary surface rupture associated with the Mw 7.1 16 October 1999 Hector Mine earthquake, San Bernardino County, California, *Bulletin of the Seismological Society of America* **92**, 1171–1191.

Vidale, J. E. and O. Bonamassa (1994). Influence of near-surface geology on the direction of ground motion above a frequency of 1 Hz. In R. Borcherdt (Ed.), *The Loma Prieta, California, Earthquake of October 17, 1989 – Strong Ground Motion*, A61–A66. U.S. Geological Survey.

Watson-Lamprey, J. A. and D. M. Boore (2007). Beyond Sa_{GMRot} : Conversion to Sa_{Arb} , Sa_{SN} , and Sa_{MaxRot} , *Bulletin of the Seismological Society of America* **97**, 1511–1524.